



# Nanoscale polarization relaxation of epitaxial BiFeO<sub>3</sub> thin film

Weigang Chen, Lu You, Gaofeng Chen, Ngeah Theng Chua, Ong Hock Guan, Xi Zou, Junling Wang, Lang Chen\*

School of Materials Science and Engineering, Nanyang Technological University, Singapore 639798, Singapore

## ARTICLE INFO

Available online 8 April 2010

### Keywords:

Polarization relaxation  
Bismuth ferrite  
Ferroelectricity  
Piezoresponse force microscopy

## ABSTRACT

The polarization relaxation phenomenon in a 40-nm-thick epitaxial BiFeO<sub>3</sub> thin film grown on a (001) SrTiO<sub>3</sub> substrate with SrRuO<sub>3</sub> bottom electrode, was studied in nanoscale using dual-frequency resonance-tracking piezoresponse force microscopy. The as-grown film shows highly irregular mosaic domain pattern. The nucleation of reversed domains followed by domain wall propagation and domain coalesce was observed during relaxations. The polarization relaxation follows a stretched exponential model  $f = 1 - e^{-k(t-t_0)^n}$  with parameters  $t_0 = 2894$  s,  $n = 0.50$  and  $k = 6.04e-4$ . Local polar defects act as nucleation centers and the time-dependent depolarization field is the driving force for polarization relaxation.

Crown Copyright © 2010 Published by Elsevier B.V. All rights reserved.

## 1. Introduction

Ferroelectric thin film has drawn tremendous attention in the last ten years due to its possible applications such as non-volatile random-access memories, high-density data storage and electromechanical sensors and microactuators [1–3]. The polarization relaxation phenomenon, which refers to the “progressive loss of polarization” in ferroelectric thin films in the absence of external electric field, has non-negligible impact on the device reliability and retention [4]. With the increase of storage density (up to 230 Gbit cm<sup>−2</sup>), the ferroelectric domains which serve as basic storage elements will be smaller and reach nanoscale [5]. Thus, it is of significant importance to understand the dynamics of polarization relaxation process at nanoscale.

The traditional way of relaxation study is the measurement of remnant polarization of a capacitor as a function of time. Due to the macroscopic size of the electrodes (typically several tens of micrometers), it is impossible to study relaxation behavior in nanoscale. Another way is using piezoresponse force microscopy (PFM), which is capable of image and modify the ferroelectric domain structures of thin film samples [6–8]. Compared with traditional capacitor-based measurement, PFM technique has the advantages of visualizing the nanoscale nucleation and domain evolution in nanoscale [9,10].

Several studies were reported about relaxations in different ferroelectric thin films, including Pb(Zr<sub>x</sub>Ti<sub>1−x</sub>)O<sub>3</sub> ( $x = 0.2$ ), PZT(40/60), and BaTiO<sub>3</sub>. Based on the study of PZT(20/80) thin films, Ganpule et al. proposed a nucleation and growth of reverse domain model with built-in electric field due to the asymmetry of electrodes as the driving force [11–13]. The relaxation process shows several characteristics including writing voltage dependence, domain faceting and domain wall pinning

and bowing out. D. Kim et al. [14] studied the relaxation behavior of a SrRuO<sub>3</sub>/BaTiO<sub>3</sub>/SrRuO<sub>3</sub> capacitor and concluded that the relaxation is caused by a large depolarization field  $E_d$  inside the ultrathin ferroelectric thin films. Fu et al.'s research of PZT(30/70) thin film on Pt/Ti/SiO<sub>2</sub>/Si substrate also indicates the depolarization field as the driving force [15]. Furthermore, W. Ahn et al. observed only domain wall motion with no nucleation of reverse domains in a 200-nm PbTiO<sub>3</sub> thin film [16]. They proposed that the driving forces of relaxation were the curved domain walls and compressive strain in *c* domains. However rare information can be found about the relaxation in the widely studied multiferroic bismuth ferrite thin films [17]. BiFeO<sub>3</sub> (BFO) is currently the only single phase material that possesses coexisting ferroelectric and magnetic (antiferromagnetic) ordering at room temperature [18]. The large value of intrinsic polarization has been confirmed in both thin film [18] and single crystal BFO samples [19]. The domain pattern and domain orientation of BFO thin films grown on different substrates have been detailed investigated by several research groups with PFM [20–23]. The objective of this paper is the visualization and dynamic analysis of nanoscale polarization relaxation behavior of epitaxial BFO thin film using DFRT-PFM.

## 2. Experiment procedure

A 40-nm-thick epitaxial BFO film was grown on a (001)-oriented SrTiO<sub>3</sub> single crystal substrate by pulsed laser deposition (PLD), with a 40-nm-thick SrRuO<sub>3</sub> layer as the bottom electrode. BFO thin film was deposited at 700 °C and 100-mTorr oxygen partial pressure using a KrF excimer laser ( $\lambda = 248$  nm) with an energy density of  $\sim 0.8$  J/cm<sup>2</sup> and 3 Hz frequency. The purity and epitaxial growth of the film was confirmed by the presence of only (00*l*) reflections in the  $\theta$ – $2\theta$  diffraction pattern using a high-resolution X-ray diffractometer (Panalytical X-pert Pro) (data not shown).

A commercial atomic force microscope (Asylum Research MFP-3D) was employed to do the piezoresponse imaging and domain

\* Corresponding author. Tel.: +65 63168980; fax: +65 67909081.

E-mail address: [LangChen@ntu.edu.sg](mailto:LangChen@ntu.edu.sg) (L. Chen).

modification of the sample. Two types of tips were used: a Pt-coated conductive silicon tip with a small spring constant of  $\sim 2$  N/m (so called “soft tip”) and a Pt/Ir-coated highly doped silicon tip with a large spring constant of  $\sim 42$  N/m (so called “hard tip”). A dual-frequency resonant-tracking piezoresponse force microscopy (DFRT-PFM) method proposed by B. Rodriguez et al. [24] was employed. As shown in Fig. 1, two AC voltages with frequencies near the same resonance are applied to the cantilever. The contact resonance frequency is tracked by analyzing the difference between the amplitudes at these two frequencies. The spatial variability of driving frequency enhances the piezoresponse signal intensity and increase image resolution by avoiding crosstalk between the contact stiffness and the piezoresponse signal. In this study, we focused on the relaxation of out-of-plane polarization, which is employed as the signal in memory and data storage applications.

A square area ( $500\text{ nm} \times 500\text{ nm}$ ) was poled with the tip grounded and  $+5\text{ V}$  DC bias applied to the bottom electrode. PFM images were recorded from the same area as a function of time. All scans were performed under ambient condition, with an AC field of  $3\text{ V}$  peak-to-peak applied to the tip. Piezoresponse phase images were carefully aligned according to the features in the topography images.

### 3. Results and discussion

As shown in Fig. 2a, the topography image of the film displayed unit-cell steps with a surface roughness of  $\sim 0.22\text{ nm}$ . Piezoresponse images were obtained by scanning the thin film with both the soft and hard tips in the same PFM system in different modes. The PFM images scanned with the hard Pt/Ir-coated highly doped silicon tip (Fig. 2d) show weak

phase contrast and blurry domain patterns, even with a high excitation  $V_{ac}$  up to  $4\text{ V}$ . The PFM images scanned by a soft Pt-coated silicon tip (Fig. 2c) with excitation AC frequency fixed at  $285\text{ kHz}$ , show improved phase contrast but the resolution is still not acceptable. In contrast, the PFM image scanned by the soft tip (Fig. 2b) using the DFRT-PFM technique shows clear phase contrast and high-resolution domain patterns, even with a smaller excitation  $V_{ac}$  ( $1.5\text{ V}$ ). The piezoresponse amplitude signal of PFM images scanned by the soft tip is much larger than that scanned by the hard tip (figure not shown). For a  $40\text{-nm}$ -thick BFO thin film, it is important to get a sharp piezoresponse image with low excitation voltage, because large voltage may affect the domain relaxation process or even partially switch domains underneath the tip. Here the DFRT-PFM is proved to be a suitable technique for domain pattern and relaxation study of BFO thin films.

The piezoresponse image (Fig. 2b) of the as-grown BFO film shows highly irregular mosaic domain structures. Because of the built-in electric field caused by electrode asymmetry (with  $\text{SrRuO}_3$  layer as bottom electrode and no top electrode), a majority of the film shows downward polarization (purple color). As reviewed by G. Catalan and J.F. Scott [17], the appearance of mosaic domains with high-density elastically costly domain walls, instead of single domain or stripe domains, indicates that the film possesses either a random distribution of defects and/or low crystal anisotropy [23]. Here low crystal anisotropy can be excluded because the BFO film is fully epitaxial with  $(001)_c$  orientation. In this respect, the reason for mosaic domain is the distribution of defects which alternates local built-in electric field and favors opposite polarity.

Fig. 3a shows the piezoresponse image scanned right after poling. A uniform yellow square corresponding to upward polarization was

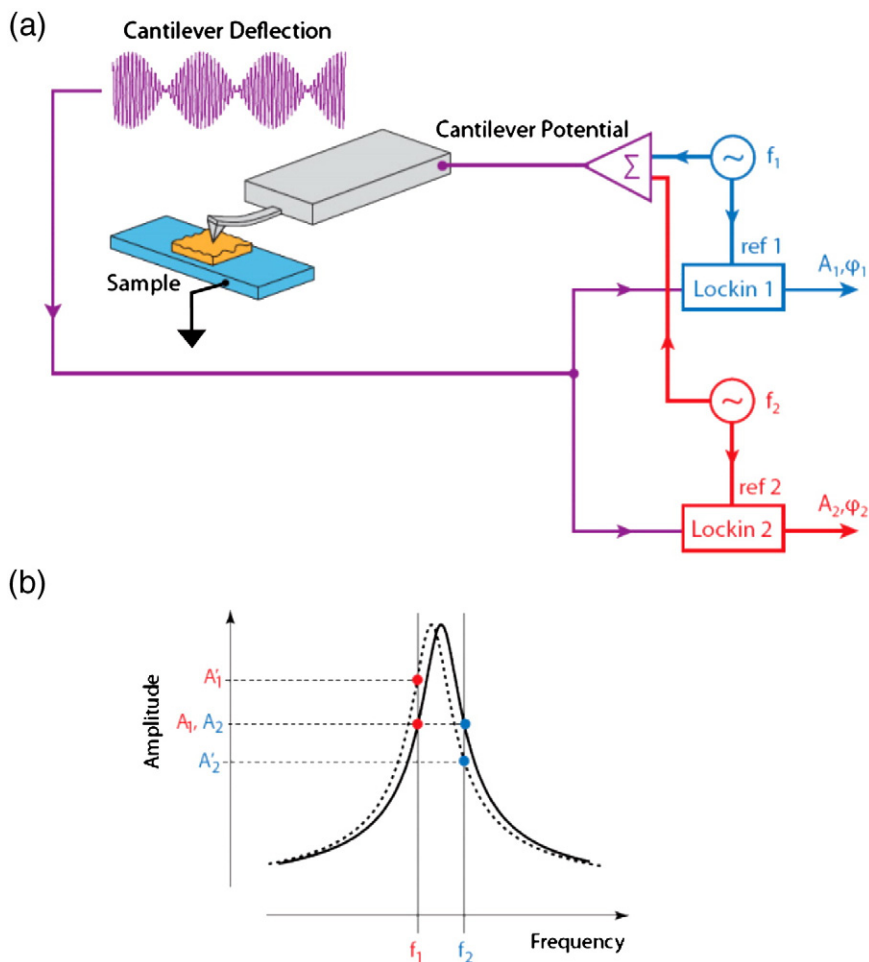
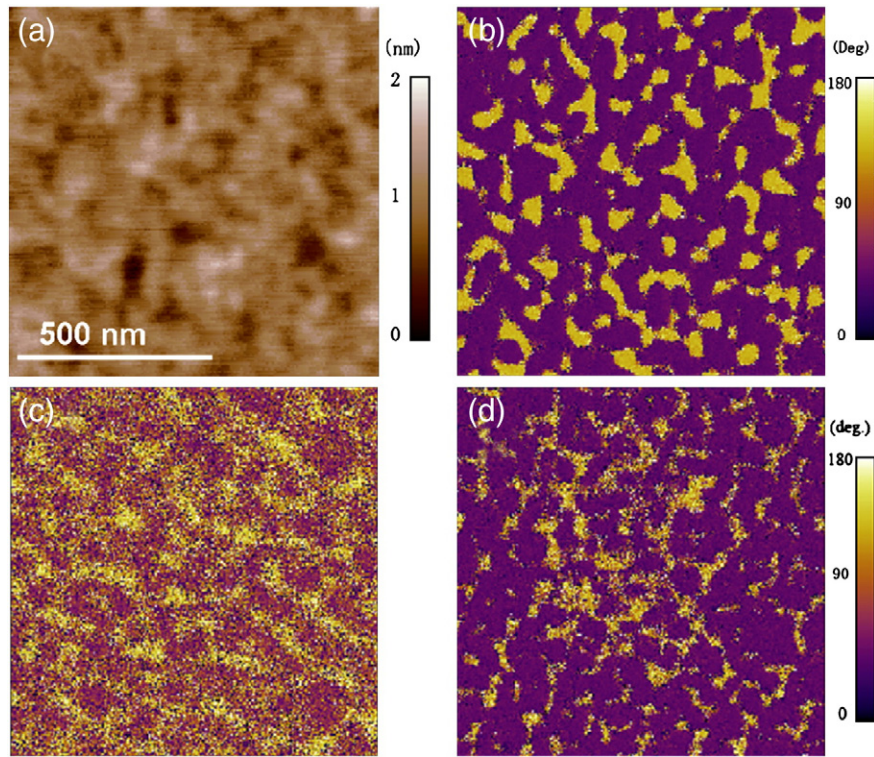
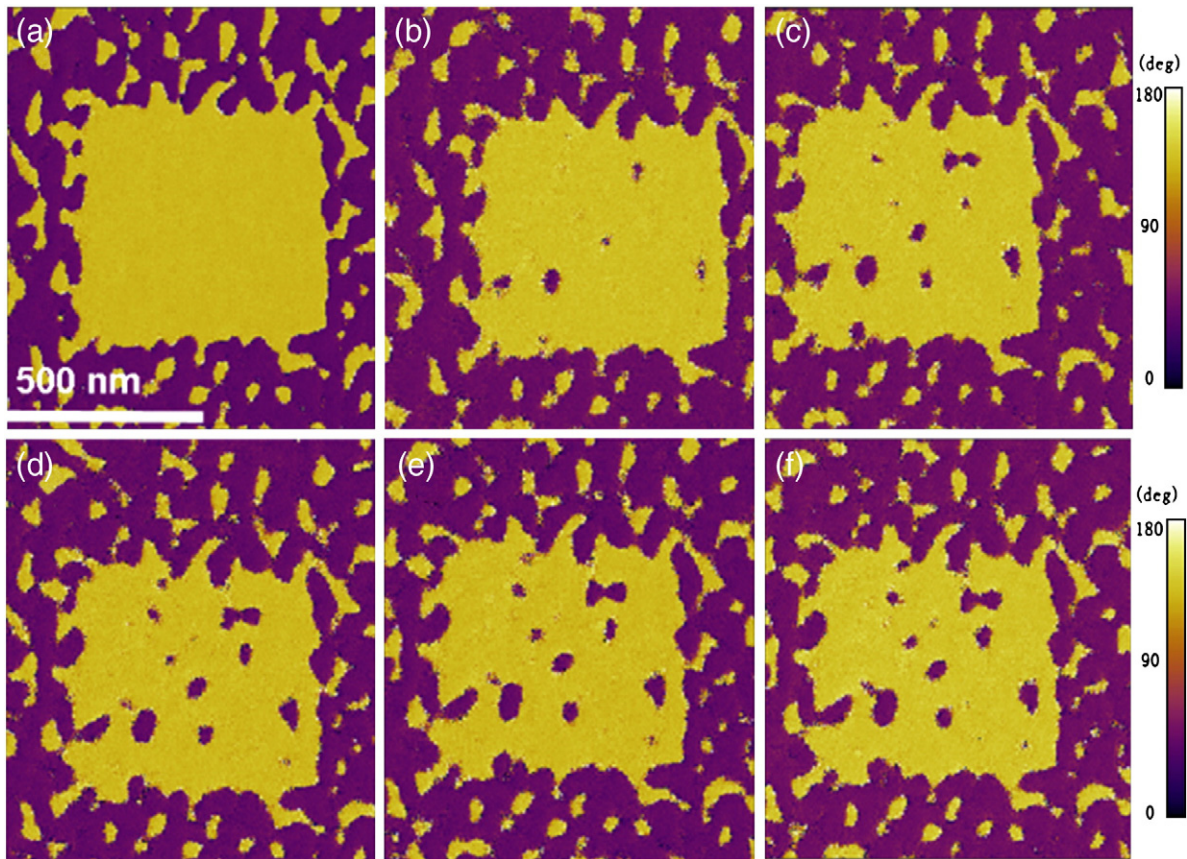


Fig. 1. Schematic diagram of Asylum Research's DFRT-PFM showing a drive phase independent feedback signal. Reprinted with permission from [24].





**Fig. 2.** Topography (a) and piezoresponse (b) images from a  $1\text{-}\mu\text{m} \times 1\text{-}\mu\text{m}$  area of the BFO sample scanned by a soft tip using DFRT-PFM mode with  $V_{ac} = 1.5\text{ V}$ . (c) Piezoresponse image scanned by a soft tip using a fixed driving frequency  $f = 285\text{ kHz}$  with  $V_{ac} = 1.5\text{ V}$ . (d) Piezoresponse image scanned by a hard tip using a fixed driving frequency  $f = 50\text{ kHz}$  with  $V_{ac} = 4\text{ V}$ .



**Fig. 3.** Piezoresponse images from a  $1\text{-}\mu\text{m} \times 1\text{-}\mu\text{m}$  area of the BFO sample showing the center yellow region which the polarization was switched upward. Images scanned with waiting time: (a) 240 s, (b) 7080 s, (c) 18,180 s, (d) 27,000 s, (e) 34,920 s, and (f) 41,580 s.

created and surrounded by mosaic as-grown domains. Fig. 3b–f shows the time evolution of the domain structure. It is clear that the relaxation process is the nucleation of reversed domains followed by propagation of the domain wall and coalesces of domains. The nucleation of reversed domains shows random sites distribution, which can be attributed to the distribution of polar defects as discussed below. Local defects with polarity and charge, such as bismuth and oxygen vacancies, break the energetic symmetry between two equivalent polarization states, leading to favorite of one particular polarization direction (random field). In this respect, local defects with polarity opposite to the poling electric field will facilitate nucleation of reversed domains and act as local nucleation centers. This is consistent with the work of S. Jesse et al. who demonstrated that polar defects will lead to unequal positive and negative nucleation bias by mapping the nucleation centers of an epitaxial PZT thin film with switching spectroscopy piezoresponse force microscopy (SS-PFM) [10].

Fig. 4a plotted the overall fraction of reversed domains in the 500-nm × 500-nm area as a function of time in 12 h. A stretched exponential model was employed to analyze the relaxation dynamics:

$$f = 1 - e^{-k(t-t_0)^n}$$

where  $f$  is the fraction of reversed domain calculated from the PFM phase image.  $t_0$ ,  $n$  and  $k$  are the fitting parameters.  $t_0$  is identified as the waiting time for reversed domain nucleation and growth to a critical size. The model is consistent with Ganpule et al.'s study [13] of PZT(20/80) thin films and Hong et al.'s study [25] of PZT(53/47) thin films. The fitting parameters of the BFO sample ( $t_0 = 2894$  s,  $n = 0.50$  and  $k = 6.04 \times 10^{-4}$ ) agree well with that of ( $t_0 = 2329$  s,  $n = 0.34$  and  $k = 0.012$ ) [13]. The similarity of the our results in BFO sample with that of PZT(20/80) thin film studied by Ganpule et al. [13] indicates

that the nucleation and growth of reversed domains governs the relaxation in both BFO and PZT films. However, instead of 90° domain walls in PZT thin film, the polar defects in BFO thin film act as the nucleation centers.

Fig. 4b plotted the domain size as a function of time for four reversed domains which were labeled in Fig. 4c. The growth of individual domains can be divided into four steps. Step 1 is the nucleation waiting period (shown as “OA” in Fig. 4b) during which a reverse domain nucleates and grows to a critical size that can be visualized in our PFM system. A distribution of nucleation waiting time range from 2500 s to 12,500 s was shown, which can be understood as a distribution of activation energies due to localized defects. In step 2 (“AB” in Fig. 4b), domain sizes increase sharply right after nucleation, which indicates a large domain wall propagation speed. In following step 3 and step 4 (“BC” and “CD” in Fig. 4b), a slow increase and finally saturation of domain sizes were observed, indicating a time-dependent domain wall propagation speed. During relaxation, the net charge at the top and bottom surfaces decreases, leading to a time-dependent depolarization field which is the driving force of the relaxation.

#### 4. Concluding remarks

In summary, the as-grown domain structure and polarization relaxation in an epitaxial BFO thin film with SrRuO<sub>3</sub> bottom electrode was investigated. The irregular mosaic as-grown domain pattern indicates a random distribution of polar defects. The relaxation process was observed as the nucleation of reversed domains followed by domain wall propagation and domain coalesce was observed during relaxation. The polarization relaxation of BFO thin film follows a stretched exponential law. Local defects act as nucleation centers and the depolarization field is the driving force for polarization relaxation.

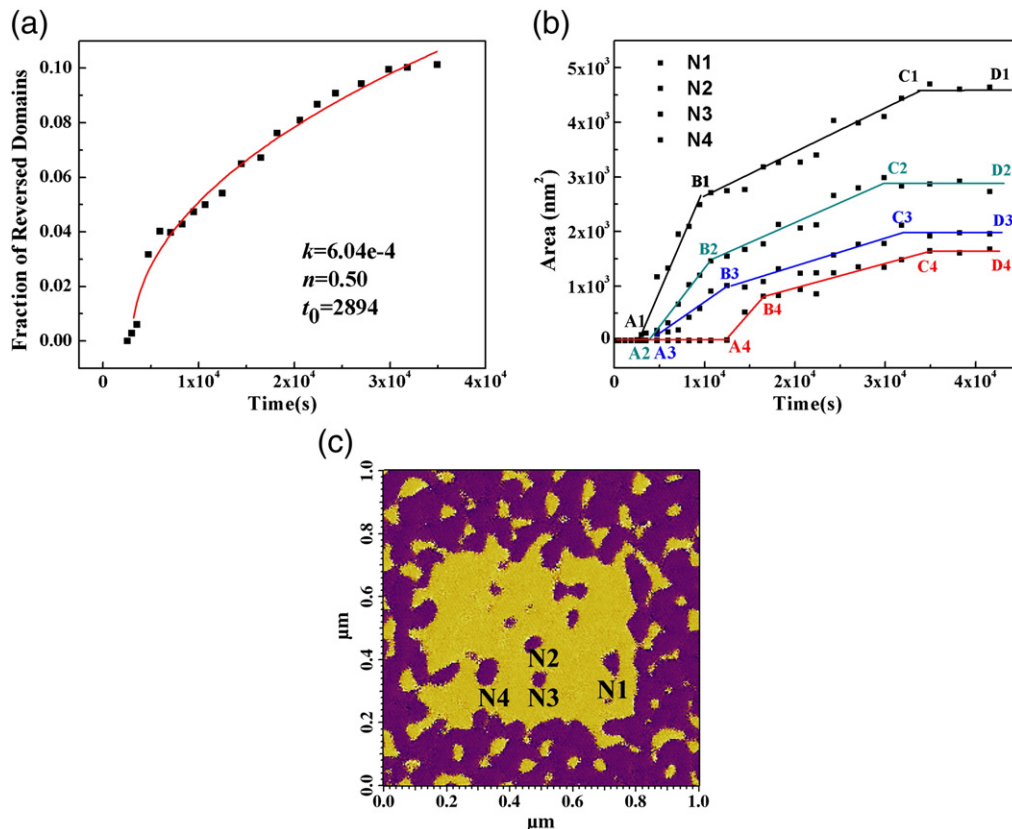


Fig. 4. (a) Fraction of reversed domains plotted as a function of time for a 1-μm × 1-μm area. (b) Domain sizes plotted as a function of time for several individual reversed domains. (c) Domains marked with N1, N2, N3 and N4 in the PFM image.

## Acknowledgements

The authors acknowledge the support from Nanyang Technological University and Ministry of Education of Singapore under project number SUG 13/06, RG 21/07 and Tier2 ARC 16/08.

## References

- [1] B.H. Park, B.S. Kang, S.D. Bu, T.W. Noh, J. Lee, W. Jo, *Nature* 401/6754 (1999) 682.
- [2] J.F. Scott, C.A.P. Dearaujo, *Science* 246/4936 (1989) 1400.
- [3] J.F. Scott, *Ferroelectrics* 314/1 (2005) 207.
- [4] N. Setter, D. Damjanovic, L. Eng, G. Fox, S. Gevorgian, S. Hong, A. Kingon, H. Kohlstedt, N.Y. Park, G.B. Stephenson, I. Stolitchnov, A.K. Taganstev, D.V. Taylor, T. Yamada, S. Streiffer, *J. Appl. Phys.* 100/5 (2006) 051606.
- [5] C. Yasuo, et al., *Nanotechnology* 17/7 (2006) S137.
- [6] A. Gruverman, O. Auciello, H. Tokumoto, *Annu. Rev. Mater. Sci.* 28/1 (1998) 101.
- [7] C. Harnagea, M. Alexe, D. Hesse, A. Pignolet, *Appl. Phys. Lett.* 83/2 (2003) 338.
- [8] J. Stephen, et al., *Nanotechnology* 17/6 (2006) 1615.
- [9] S.V. Kalinin, B.J. Rodriguez, S. Jesse, E. Karapetian, B. Mirman, E.A. Eliseev, A.N. Morozovska, *Annu. Rev. Mater. Sci.* 37/1 (2007) 189.
- [10] S. Jesse, B.J. Rodriguez, S. Choudhury, A.P. Baddorf, I. Vrejoiu, D. Hesse, M. Alexe, E.A. Eliseev, A.N. Morozovska, J. Zhang, L.-Q. Chen, S.V. Kalinin, *Nat. Mater.* 7/3 (2008) 209.
- [11] C.S. Ganpule, A.L. Roytburd, V. Nagarajan, B.K. Hill, S.B. Ogale, E.D. Williams, R. Ramesh, J.F. Scott, *Phys. Rev. B Condens. Matter Mater. Phys.* 65/1 (2001) 014101.
- [12] C.S. Ganpule, V. Nagarajan, H. Li, A.S. Ogale, D.E. Steinhauer, S. Aggarwal, E. Williams, R. Ramesh, P. De Wolf, *Appl. Phys. Lett.* 77/2 (2000) 292.
- [13] C.S. Ganpule, V. Nagarajan, S.B. Ogale, A.L. Roytburd, E.D. Williams, R. Ramesh, *Appl. Phys. Lett.* 77/20 (2000) 3275.
- [14] D.J. Kim, J.Y. Jo, Y.S. Kim, Y.J. Chang, J.S. Lee, J.-G. Yoon, T.K. Song, T.W. Noh, *Phys. Rev. Lett.* 95/23 (2005) 237602.
- [15] D. Fu, K. Suzuki, K. Kato, H. Suzuki, *Appl. Phys. Lett.* 82/13 (2003) 2130.
- [16] W.S. Ahn, W.W. Jung, S.K. Choi, Y. Cho, *Phys. Rev. Lett.* 88/8 (2006) 082902.
- [17] G. Catalan, J.F. Scott, *Adv. Mater.* 21/24 (2009) 2463.
- [18] J. Wang, J.B. Neaton, H. Zheng, V. Nagarajan, S.B. Ogale, B. Liu, D. Viehland, V. Vaithyanathan, D.G. Schlom, U.V. Waghmare, N.A. Spaldin, K.M. Rabe, M. Wuttig, R. Ramesh, *Science* 299/5613 (2003) 1719.
- [19] D. Lebeugle, D. Colson, A. Forget, M. Viret, P. Bonville, J.F. Marucco, S. Fusil, *Phys. Rev. B Condens. Matter Mater. Phys.* 76/2 (2007) 024116.
- [20] F. Zavaliche, P. Shafer, R. Ramesh, M.P. Cruz, R.R. Das, D.M. Kim, C.B. Eom, *Appl. Phys. Lett.* 87/25 (2005) 252902.
- [21] Y.H. Chu, Q. Zhan, L.W. Martin, M.P. Cruz, P.L. Yang, G.W. Pabst, F. Zavaliche, S.Y. Yang, J.X. Zhang, L.Q. Chen, D.G. Schlom, I.N. Lin, T.B. Wu, R. Ramesh, *Adv. Mater.* 18/17 (2006) 2307.
- [22] F. Zavaliche, S.Y. Yang, T. Zhao, Y.H. Chu, M.P. Cruz, C.B. Eom, R. Ramesh, *Phase Transit.* 79/12 (2006) 991.
- [23] G. Catalan, H. Bea, S. Fusil, M. Bibes, P. Paruch, A. Barthelemy, J.F. Scott, *Phys. Rev. Lett.* 100/2 (2008) 027602.
- [24] B.J. Rodriguez, et al., *Nanotechnology* 18/47 (2007) 475504.
- [25] J.W. Hong, W. Jo, D.C. Kim, S.M. Cho, H.J. Nam, H.M. Lee, J.U. Bu, *Appl. Phys. Lett.* 75/20 (1999) 3183.